All-printed Strain Sensors: Building Blocks of the Aircraft Structural Health Monitoring System

Yuzheng Zhang[a,b], Nickolas Anderson[c], Scott Bland[a], Steven Nutt[b], Gregory Jursich[c], and Shiv Joshi[a]

a. NextGen Aeronautics Inc.,
2780 Skypark Drive, Suite 400
Torrance, CA 90505, USA

b. Department of Chemical Engineering and Materials Science,
University of Southern California,
Los Angeles, CA90089, USA

c. Department of Bioengineering,
University of Illinois at Chicago,
Chicago, IL60607, USA

Corresponding author:
Yuzheng Zhang
E-mail: yzheng@nextgenaero.com
Telephone: 1(310)626-8360

Abstract:

Characterization of all-printed strain gages to assess their suitability for structural state monitoring of large structures is presented. Strain sensor response, transverse strain sensitivity and long-term reliability are key performance parameters of printed strain sensors on flexible substrates. These key performance parameters are evaluated for inkjet and screen printed strain sensors on polyethylene-terephthalate (PET) flexible substrates. More specifically, printing characteristics of commercially available inks, gage factor of serpentine strain sensors with transverse strain and temperature sensitivity, and sensor

Please cite this article as: “All-printed Strain Sensors: Building Blocks of the Structural Health Monitoring System” Y Zhang, N Anderson, S Bland, S Nutt, G Jursich, and S Joshi, in press, Sensors and Actuators A, Oct (2016). DOI: 10.1016/j.sna.2016.10.007

reliability under unidirectional tensile and fatigue loading is assessed. Maximum strain to which both inkjet and screen printable formulations can be reliably used for long-term repeatable measurements is recommended based on tensile and fatigue testing. Variation in gage factor is attributed to micro- and macro-scale fracture of printed traces under mechanical loading. Substrate, ink and printing process parameters are identified to further improve strain sensing characteristics of low-cost, large area strain mapping systems. Reliable, low-cost, and large-area strain mapping systems are sought for continuous or on-demand real-time diagnosis and prognosis of complex structural components.

1. Introduction

In the past decade, innovative technologies and functional materials have been explored to develop applications of printed electronics and sensors [1, 2]. For example, an all-printed strain sensor array is a recent example of a low-cost, flexible and light-weight system that provides a reliable method for monitoring the state of aircraft components [3]. The sensor system layout, as illustrated in Figure 1, features multiple sensor arrays, power supply unit, transistors and wiring, all of which can be printed on one flexible substrate. This thin film system can be readily integrated in/on to target structures without a large weight addition. Real-time strain data output ensures onboard flight safety and allows quick diagnosis of key structural components during both operation and maintenance. The usage of this system is not limited to aviation. It is also applicable to any structure that requires real-time strain monitoring. As a key building block in this system, the strain sensor, often in a

Please cite this article as: “All-printed Strain Sensors: Building Blocks of the Structural Health Monitoring System” Y Zhang, N Anderson, S Bland, S Nutt, G Jursich, and S Joshi, in press, Sensors and Actuators A, Oct (2016). DOI: 10.1016/j.sna.2016.10.007

serpentine shape, converts strain into measurable resistance changes based on the piezoresistive effect of the ink materials [4]. The sensor's performance and durability are largely determined by the printing methods and ink/substrate materials.

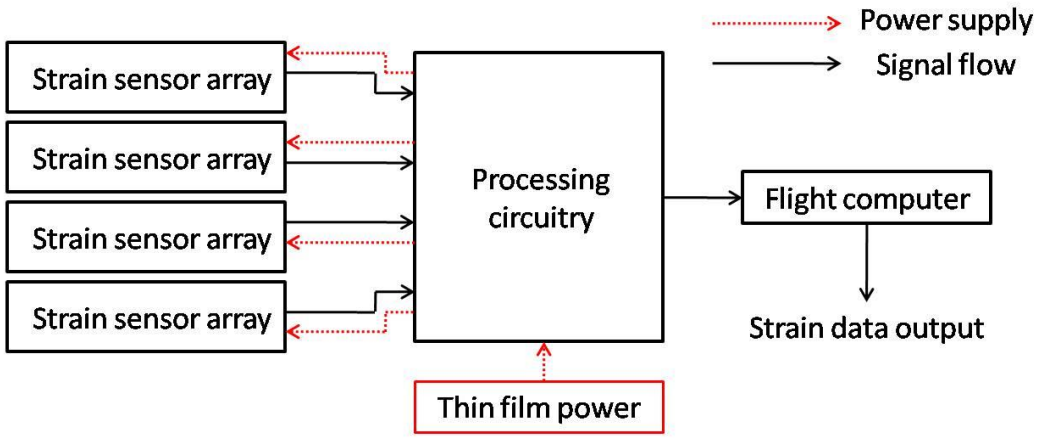

Figure 1. Illustration of an all-printed strain sensor system.

Among all-printing techniques, screen printing and inkjet printing methods are much better suited for smaller-scale prototyping and have drawn most interest due to maturity of printing procedures and availability of compatible inks and substrates. Screen printing relies on a mask (screen) to transfer a pattern onto a substrate. Screen printing is widely used because of the high printing speed, large selection of ink/substrate materials, and capability of making complex multilayer devices [5]. However, compared to ink-jet printing, it has less printing consistency, offers lower resolution, consumes more ink material, and requires expensive masks. Applications of the screen printing technique have been explored and studied in the past decade. For example, Wei reported a screen-printed capacitive cantilever beam used as a wearable motion sensor [6]. Screen-printed electrodes

Please cite this article as: "All-printed Strain Sensors: Building Blocks of the Structural Health Monitoring System" Y Zhang, N Anderson, S Bland, S Nutt, G Jursich, and S Joshi, in press, Sensors and Actuators A, Oct (2016). DOI: 10.1016/j.sna.2016.10.007

have also been widely used for biosensors [7]. In this work, a carbon-based polymer ink was used as the ink material for printed strain sensors. This graphite ink was chosen because of its high resistivity and excellent mechanical integrity. Although this graphite ink is widely available for screen printing of resistors [8, 9], its piezoresistivity for strain sensors has not been systematically studied.

On the contrary, inkjet printing is a mask-less method in which moving nozzles deposit ink drops on demand based on pattern design. The ability to print complex patterns with high spatial resolution and excellent printing consistency allows inkjet printing to be used as a rapid prototyping tool for printed electronics [10]. However, the inks for inkjet printing are currently limited to nanoparticle (NP)-based solutions due to the compatibility issue between nozzle and ink which often causes nozzle clogging [5]. Herrmann [11] described a strain gage composed of gold NPs and showed that the NP-based gage exhibited an exponential dependence of the gage resistance to applied strain due to electron tunneling between NPs. Bruno explored a cost-effective method to make prototype strain sensors using inkjet printing [5]. Borghetti studied mechanical behaviors of PEDOT:PSS and silver NP strain sensors on a polyimide substrate [10]. However, none of these studies reported the mechanical reliability (i.e. damage tolerance and fatigue resistance) of the sensors fabricated by inkjet printing. In this study, both screen printing and inkjet printing methods were utilized to make serpentine strain sensors using carbon-based polymer ink and silver NP-based ink, respectively. The performance characteristics of the printed strain sensors,

Please cite this article as: “All-printed Strain Sensors: Building Blocks of the Structural Health Monitoring System” Y Zhang, N Anderson, S Bland, S Nutt, G Jursich, and S Joshi, in press, Sensors and Actuators A, Oct (2016). DOI: 10.1016/j.sna.2016.10.007

including sensitivity, accuracy, reliability, and ink morphology, were evaluated in parallel. A structure-to-property correlation was established to reveal important characteristics of a working strain sensor.

2. Experiment procedures

2.1. Printing procedures

Screen printing and inkjet printing were used for strain sensors and investigated in parallel. The sensors were screen printed on 5-mil (127 μm) thick PET substrates (McMaster-Carr) using a bench-top manual stencil printer (Gold Print SPR-25). The PET substrates were rinsed with 2-propanol (99% ACS Grade from Aldrich) prior to printing. Subsequently, a carbon ink (DuPont 7082) serpentine pattern was screen printed (mesh count of 325 wires per inch) to the substrate using a 70 durometer squeegee blade at a printing speed of ~3 cm/s. The carbon ink was then cured in an oven at 105ºC for 30 minutes with an air flow of 15.6 L/min. A second silver contact pattern (DuPont 5028) was screen printed at a speed of ~8 cm/s and cured accordingly.

In parallel, a commercial printer (Dimatix Material Printer DMP-2381) was used to print strain sensors using the inkjet process. During inkjet printing, silver nanoparticle (NP) ink (Mitsubishi NBSIJ-FD02) was deposited on a porous alumina coated PET film (Mitsubishi NB-WF-3GF100). The waveform used for the silver nanoparticle ink was based on a standard ink (Dimatix Model Fluid) and was modified to ensure ink drop formation and a

Please cite this article as: “All-printed Strain Sensors: Building Blocks of the Structural Health Monitoring System” Y Zhang, N Anderson, S Bland, S Nutt, G Jursich, and S Joshi, in press, Sensors and Actuators A, Oct (2016). DOI: 10.1016/j.sna.2016.10.007

straight printing path with a 1 picoliter nominal drop volume. The average drop diameter is 16 μm and the drop spacing is 10 μm. Maximum voltage and jetting frequency were set to 20 V and 8 kHz for all 16 nozzles on the printhead (Dimatix DMC-11601). The inkjet and bed temperatures are 33ºC and 27ºC, respectively. The serpentine resistive strain sensors were made with two printing passes and were allowed to cure at room temperature for 24 hours. Figure 2 shows the screen-printed and inkjet-printed strain sensors on PET substrates. The screen-printed sensors tested in this work have a gage length of 8.1 mm with a line width of 340 μm. The inkjet-printed sensors have a gage length of 9.1 mm with a line width of 180 μm.

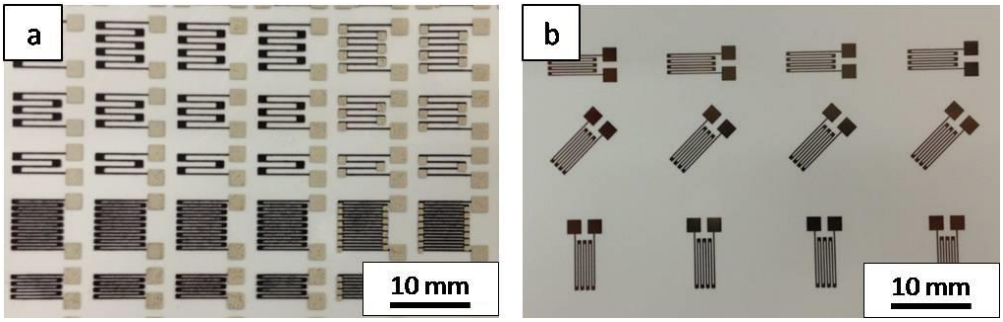

Figure 2. Images of (a) screen-printed and (b) inkjet-printed strain sensors on PET substrates.

2.2. Ink characterization

The light microscopy images were recorded using a stereo digital light microscope (Keyence VHX-600e). The microstructures of the screen-printed carbon layer and the inkjet-printed silver NPs were investigated using a field emission scanning electron

Please cite this article as: “All-printed Strain Sensors: Building Blocks of the Structural Health Monitoring System” Y Zhang, N Anderson, S Bland, S Nutt, G Jursich, and S Joshi, in press, Sensors and Actuators A, Oct (2016). DOI: 10.1016/j.sna.2016.10.007

microscope (JELO JEM 7001F) operated at 20kV. Cross sectional samples were prepared using an ion polisher (JEOL IB-09010CP).

2.3. *In situ* tensile testing

The sensitivity of a strain sensor (i.e., sensor response to applied strain) was obtained using the micro-tensile measurement apparatus shown in Figure 3(a). The printed sensors were cut into dog-bone specimens (Figure 3(b)) and quasi-statically tensile-strained at a constant rate of ~10^{-4} s^{-1}. The strain was recorded through the displacement transducer on the micro-tensile module. The change in sensor resistance was monitored *in situ* using a digital multimeter.

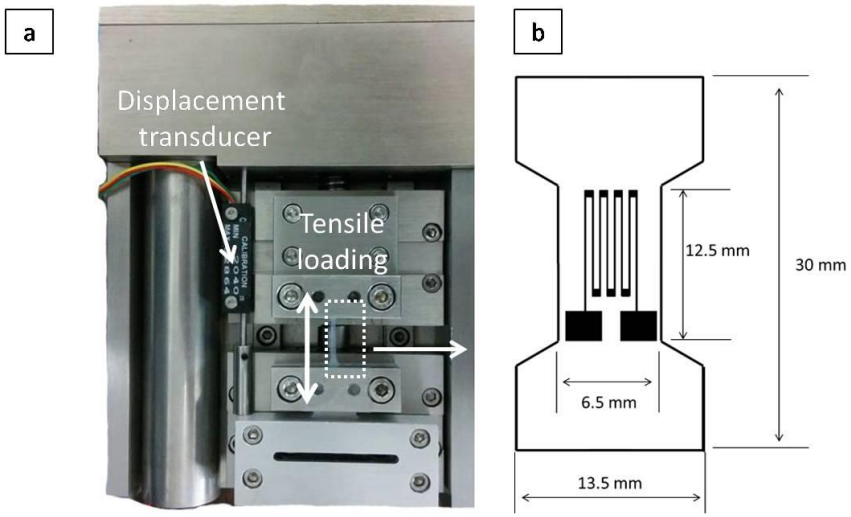

Figure 3. (a) Micro-tensile module and (b) geometry of a dog-bone specimen.

2.4. Fatigue testing

Please cite this article as: "All-printed Strain Sensors: Building Blocks of the Structural Health Monitoring System" Y Zhang, N Anderson, S Bland, S Nutt, G Jursich, and S Joshi, in press, Sensors and Actuators A, Oct (2016). DOI: 10.1016/j.sna.2016.10.007

The reliability of the sensors against cyclic loading was tested using a fatigue testing frame (Instron 8500) with a cyclic load frequency of 5 Hz. The printed sensors along with a commercial foil gage were attached to an aluminum beam. The fatigue test was carried out using a four-point bending setup. The thickness to length ratio of the aluminum beam was small enough to assume that bending was uniform between two inner adjacent bending pins. Real time strain data was measured by the calibrated commercial foil gage and collected using a data acquisition module (Micro-measurement 8000), and the resistance change of the testing gage was continuously recorded by a resistance data logger. Finally, strain and resistance data were synchronized and plotted against each other using a custom MATLAB program. This fatigue testing platform is illustrated in Figure 4.

Figure 4.Illustration of the fatigue testing platform.

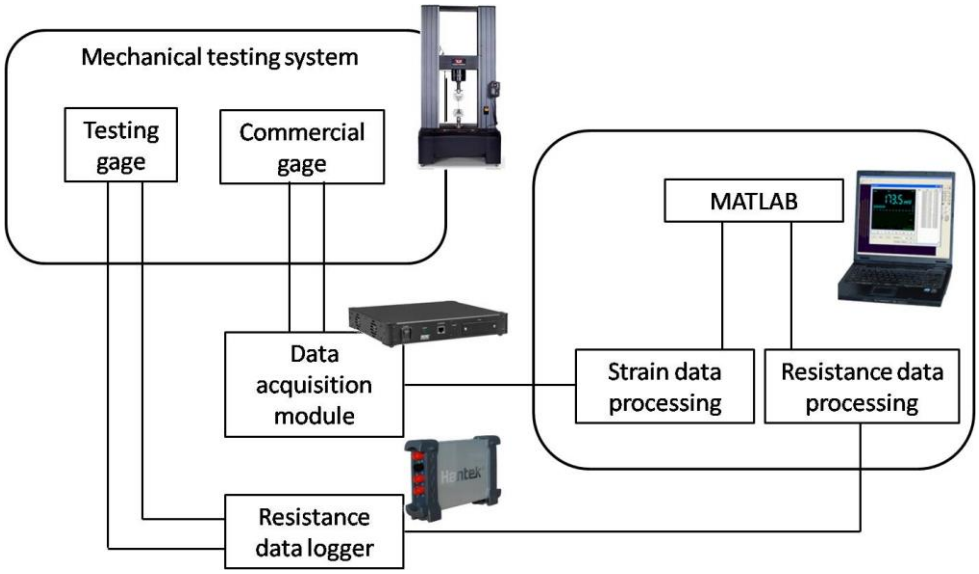

3. Results and Discussion

3.1. Ink characterization

Please cite this article as: “All-printed Strain Sensors: Building Blocks of the Structural Health Monitoring System” Y Zhang, N Anderson, S Bland, S Nutt, G Jursich, and S Joshi, in press, Sensors and Actuators A, Oct (2016). DOI: 10.1016/j.sna.2016.10.007

The performance and properties of a sensor are closely related to the microstructures of the printed layers. Figures 5 (a) and (d) show printed lines of the screen-printed and the inkjet-printed sensors, respectively. The screen-printed carbon ink had a line width of ~340 μm, while the inkjet-printed sensor exhibited a finer line width of ~180 μm. Both printing methods printed well-defined ink lines with sharp edges. However, Figure 5 (d) shows sprayed droplets present outside the inkjet-printed lines areas. This was most likely due to partial clogging of the nozzle, resulting misaligned spray pattern. In addition, as indicated by the arrow in Figure 5 (d), a defect is observed on an inkjet-printed line which is believed to be introduced by aluminum silicate impurities on the alumina coating. Figure5 (b) and (e) show the surfaces of the screen-printed and inkjet-printed sensors. The carbon ink was composed of graphite particles embedded in a polymer binder, forming a rough surface as shown in Figure 5(b). Figure 5 (c) shows the cross sectional micrograph of a carbon ink layer (~18 μm thick), indicating an absence of micro-voids or cracks in the cured carbon ink layer. The clean carbon/PET interface and void-free microstructure of the carbon ink enhanced its mechanical integrity and fatigue resistance, as reported in section 3.3. On the other hand, the inkjet-printed sensor was composed of an open-cell network of nanoparticles (~100 nm in diameter) that were loosely sintered together, as shown in Figure 5(e). The cross sectional micrograph (Figure 5(f)) shows the silver NP layer (~ 2 μm) that was deposited and cured on a PET substrate coated with a porous alumina layer (~40 μm). The interconnected pores throughout the silver layer acted as numerous crack initiation sites under loading due to stress concentrations. Although ink types used for printed electronics are limited, choosing a void-free ink with good substrate adhesion is crucial to

Please cite this article as: “All-printed Strain Sensors: Building Blocks of the Structural Health Monitoring System” Y Zhang, N Anderson, S Bland, S Nutt, G Jursich, and S Joshi, in press, Sensors and Actuators A, Oct (2016). DOI: 10.1016/j.sna.2016.10.007

the mechanical reliability of any sensor subject to cyclic stress. The porous structure of the inkjet-printed silver gage precludes use as a strain sensor, despite the advantages of inkjet printing.

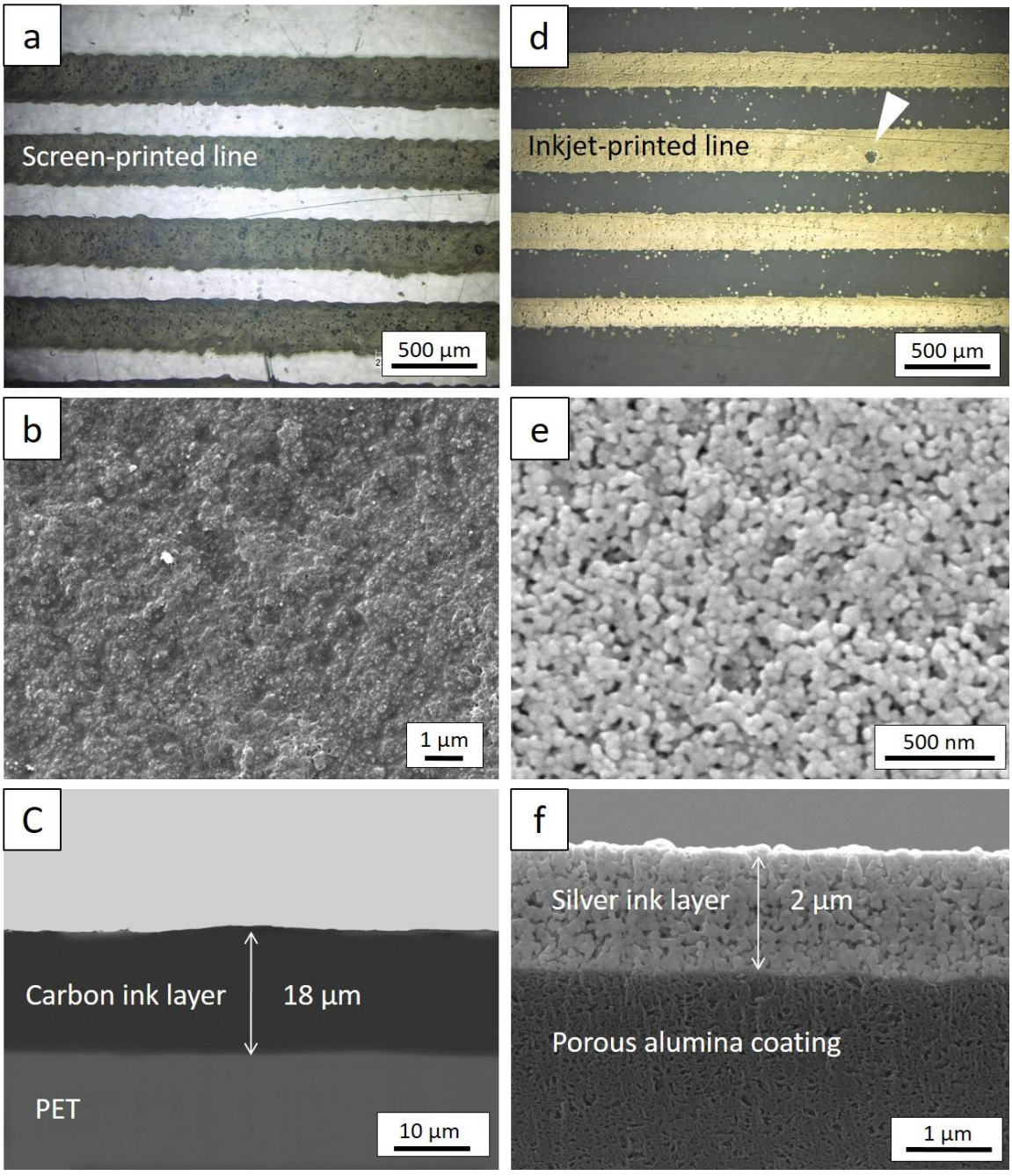

Please cite this article as: “All-printed Strain Sensors: Building Blocks of the Structural Health Monitoring System” Y Zhang, N Anderson, S Bland, S Nutt, G Jursich, and S Joshi, in press, Sensors and Actuators A, Oct (2016). DOI: 10.1016/j.sna.2016.10.007

Figure 5. (a) Light microscopy image of the screen-printed sensor (plan view), (b) surface topography of the carbon ink layer showing graphite particles embedded in polymeric binder, (c) cross sectional SEM micrograph of the screen-printed carbon ink layer deposited on a PET substrate, , (d) light microscopy image of the inkjet-printed sensor where the arrow indicates a printing defect, (d) surface of the silver NP layer, and (f) cross sectional SEM micrograph of the inkjet-printed silver NP layer printed on a PET substrate coated with alumina thin film (~40 μm).

3.2. Gage factor

The resistances of as-printed carbon and silver NP sensors were 875 kΩ and 65.2 Ω, respectively (Table 1). At least ten sensors were tested for each sensor type. The large resistance of the carbon-ink sensors has the benefit of low power consumption, reduced current-resistance (I^2R) heating, and negligible contributions from auxiliary circuitry. The inkjet-printed silver sensors exhibited small variation in resistance because of the highly repeatable and precise inkjet printing process. The carbon-ink sensors showed significant resistance variation due to inconsistent ink layer thickness from the manual screen printing process. The responses of carbon-ink and silver-ink sensors are plotted in Figures 6 (a) and (b), respectively. A 1% tensile strain was applied along the longer axis of the sensor. The sensor responses to strain were linear for both carbon-ink and silver-ink sensors within 1% strain range. A small hysteresis was observed in the tension/recovery curves of the inkjet-printed silver gage, which was an early indication of nanoparticle debonding (section 3.3).

Please cite this article as: “All-printed Strain Sensors: Building Blocks of the Structural Health Monitoring System” Y Zhang, N Anderson, S Bland, S Nutt, G Jursich, and S Joshi, in press, Sensors and Actuators A, Oct (2016). DOI: 10.1016/j.sna.2016.10.007

Gage factor *K* is defined as the ratio of resistance change to applied strain as expressed in Equation 1, where R_0 is the as-printed sensor resistance, *K* is the gage factor, and ε is the applied strain as measured by commercial strain sensor.

$$\frac{R-R_0}{R_0} = K \cdot \varepsilon \quad \text{(Equation 1)}$$

The slope of the curves in Figure 6 represents the gage factor *K*. Both the screen-printed and the inkjet-printed sensors exhibited good strain sensitivity, with gage factors of 8.8 and 3.7, respectively (Table 1), which compare favorably with commercial foil strain gages, which typically have a gage factor of 2. Note that the gage factor variance for the carbon-ink gages was insignificant, despite large scattering of resistance values in the same sample batch. In other words, the gage factor was mainly determined by ink types rather than by ink thickness.

Table 1. As-printed resistances and gage factors of the screen-printed and inkjet-printed strain sensors.

Ink type	Printing method	Resistance (as-printed)	Gage factor K
Carbon paste	Screen	875 kΩ ± 514 kΩ	8.8 ± 0.3
Silver NP	Inkjet	65.2Ω ± 0.3 Ω	3.7 ± 0.3

Please cite this article as: "All-printed Strain Sensors: Building Blocks of the Structural Health Monitoring System" Y Zhang, N Anderson, S Bland, S Nutt, G Jursich, and S Joshi, in press, Sensors and Actuators A, Oct (2016). DOI: 10.1016/j.sna.2016.10.007

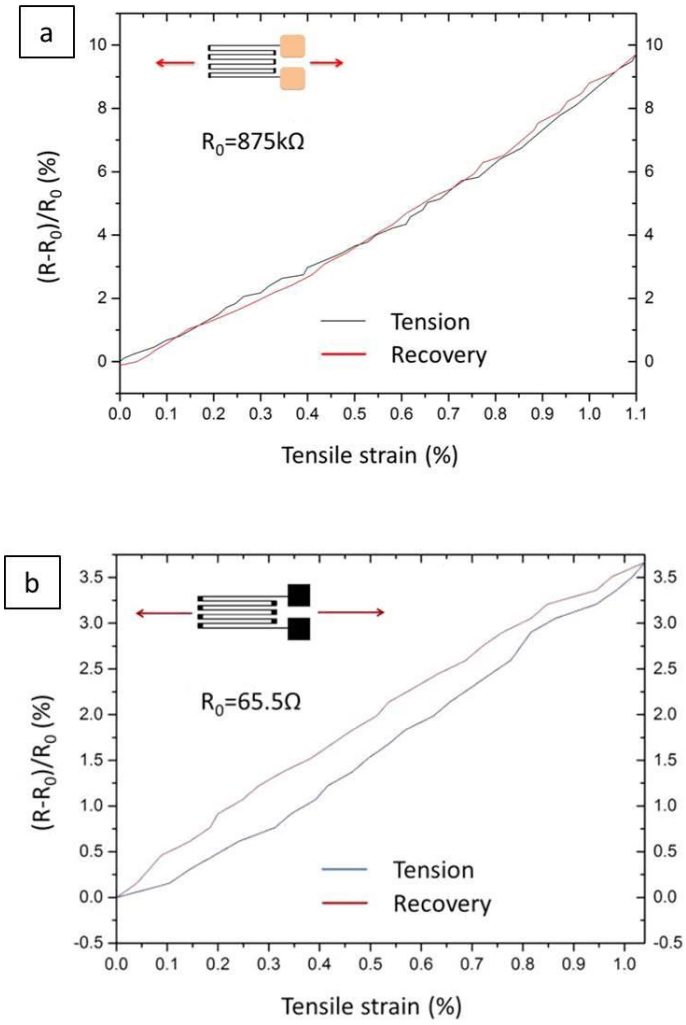

Figure 6. Sensor response curves of (a) screen-printed sensor, and (b) inkjet-printed sensor.

3.3. Sensor reliability

The use of a strain sensor would be limited should it fail to endure strains during operation. The printed sensors were a special concern because new fabrication methods and

Please cite this article as: "All-printed Strain Sensors: Building Blocks of the Structural Health Monitoring System" Y Zhang, N Anderson, S Bland, S Nutt, G Jursich, and S Joshi, in press, Sensors and Actuators A, Oct (2016). DOI: 10.1016/j.sna.2016.10.007

substrate/ink systems were being explored. The max strain without causing unrecoverable damage was described as "strain tolerance level" in the current context [12]. During tensile tests, the strain range was set from zero to a maximum tensile strain level. The gage factor was continuously monitored as the max strain level was increased. In these measurements, an abrupt gage factor increase indicates sensor damage due to crack formation and propagation.

Figure 7 shows the sensor response curves of the screen-printed and the inkjet-printed sensors. Figure 7 (a) shows that the response curves of the screen-printed sensors were linear and repeatable up to 0.9% strain, indicating a strain tolerance level below 0.9%. On the contrary, the inkjet-printed sensors showed an early deviation from linearity at ~0.2% strain (Figure 7 (b)). As the maximum strain level increased, the response curves of the inkjet-printed sensor became less linear as a result of micro-crack propagation. The insert of Figure 7 (b) shows evidence of micro-crack formation and propagation as a result of applied strain (~0.1%). These micro-cracks were immediate damage in strained silver NP layer as opposed to accumulated fatigue damage.

Please cite this article as: "All-printed Strain Sensors: Building Blocks of the Structural Health Monitoring System" Y Zhang, N Anderson, S Bland, S Nutt, G Jursich, and S Joshi, in press, Sensors and Actuators A, Oct (2016). DOI: 10.1016/j.sna.2016.10.007

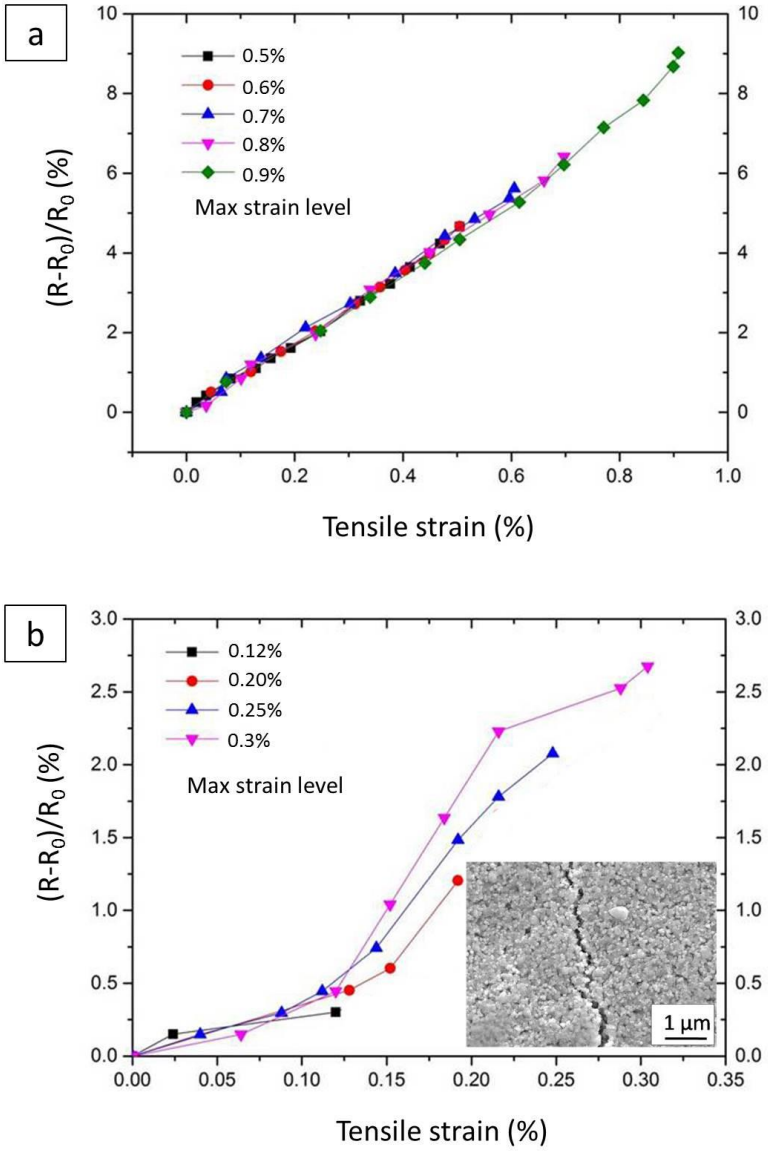

Figure 7. The sensor response curves as a function of applied strain of (a) the screen-printed sensor and (b) the inkjet-printed sensor where the insert shows a micro-crack propagating through the surface of the silver NP ink.

In addition to strain tolerance level, fatigue resistance of the carbon-ink sensors was evaluated up to 10^5 loading cycles. Because the elastic strain that most engineering

Please cite this article as: "All-printed Strain Sensors: Building Blocks of the Structural Health Monitoring System" Y Zhang, N Anderson, S Bland, S Nutt, G Jursich, and S Joshi, in press, Sensors and Actuators A, Oct (2016). DOI: 10.1016/j.sna.2016.10.007

structures experience during operation is usually small, the cyclic tensile strain was set from 0 to 0.2 %, which is well below the strain tolerance level (~0.9%) of the screen-printed sensor. Figure 8 (a) shows the sensor response curves measured at different stages of the fatigue test. The response curves were linear and repeatable during cyclic loading. Figure 8 (b) shows a small gage factor variation (±1.2%), indicating the carbon-ink sensors to be fatigue resistant up to 10^5 loading cycles. To summarize, high strain tolerance level and the fatigue resistance of the carbon-ink strain sensors delivered performance consistency and extended life-time that the silver-ink sensors were unable to achieve.

Please cite this article as: “All-printed Strain Sensors: Building Blocks of the Structural Health Monitoring System” Y Zhang, N Anderson, S Bland, S Nutt, G Jursich, and S Joshi, in press, Sensors and Actuators A, Oct (2016). DOI: 10.1016/j.sna.2016.10.007

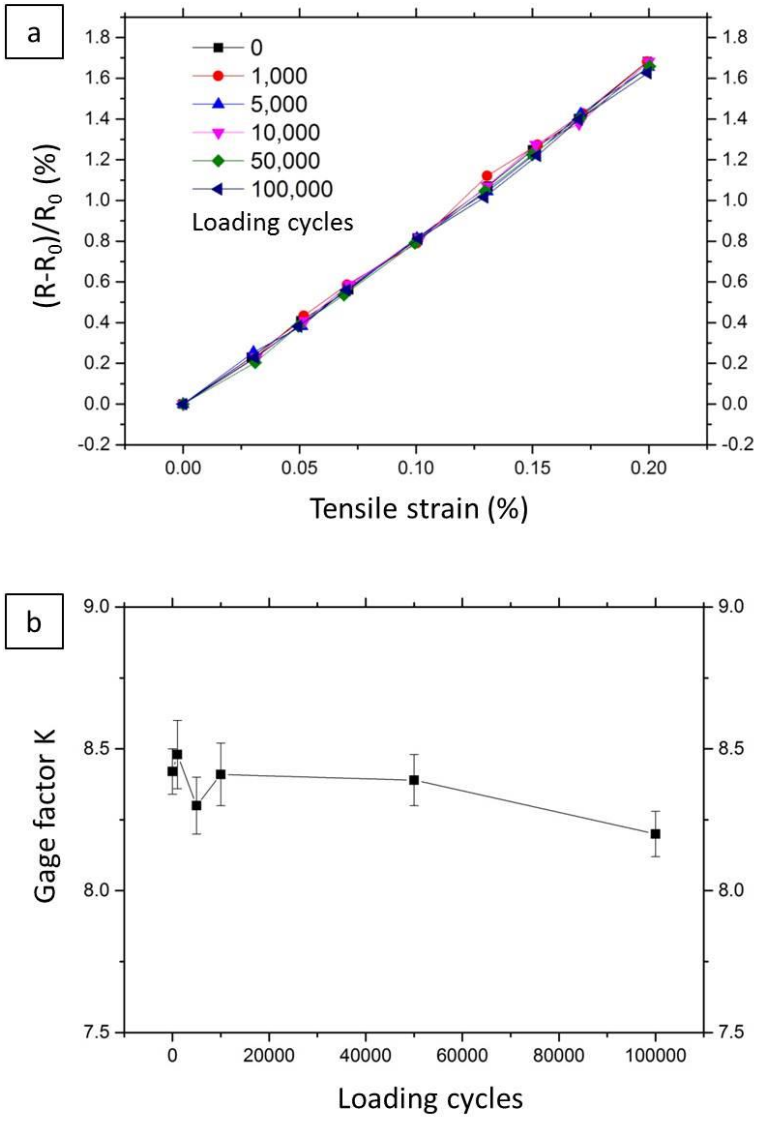

Figure 8. (a) Sensor response curves of the screen-printed sensor measured at different fatigue cycles, and (b) The gage factor variation of the screen-printed sensor as a function of loading cycles.

3.4. Transverse sensitivity

Please cite this article as: "All-printed Strain Sensors: Building Blocks of the Structural Health Monitoring System" Y Zhang, N Anderson, S Bland, S Nutt, G Jursich, and S Joshi, in press, Sensors and Actuators A, Oct (2016). DOI: 10.1016/j.sna.2016.10.007

Ideally, a strain sensor should be sensitive only to unidirectional strain along its longer axis in order to separate plane strains in X and Y directions. Thus, a serpentine circuit design is often used in commercial strain gages in order to minimize signal response from transverse loading. Transverse sensitivity, defined as the ratio of the gage factor in the transverse direction to the gage factor in the longitudinal direction, is used to evaluate sensor accuracy in measuring unidirectional strain [13]. The sensor response curves in both longitudinal and transverse directions are shown in Figure 9 for the screen-printed and inkjet-printed sensors. The transverse sensitivities of each sensor type are summarized in Table 2. The screen-printed and the inkjet-printed strain sensors showed much greater transverse sensitivities (52% and 31%, respectively) compared to the commercial foil gage (typically less than 1%).

Please cite this article as: "All-printed Strain Sensors: Building Blocks of the Structural Health Monitoring System" Y Zhang, N Anderson, S Bland, S Nutt, G Jursich, and S Joshi, in press, Sensors and Actuators A, Oct (2016). DOI: 10.1016/j.sna.2016.10.007

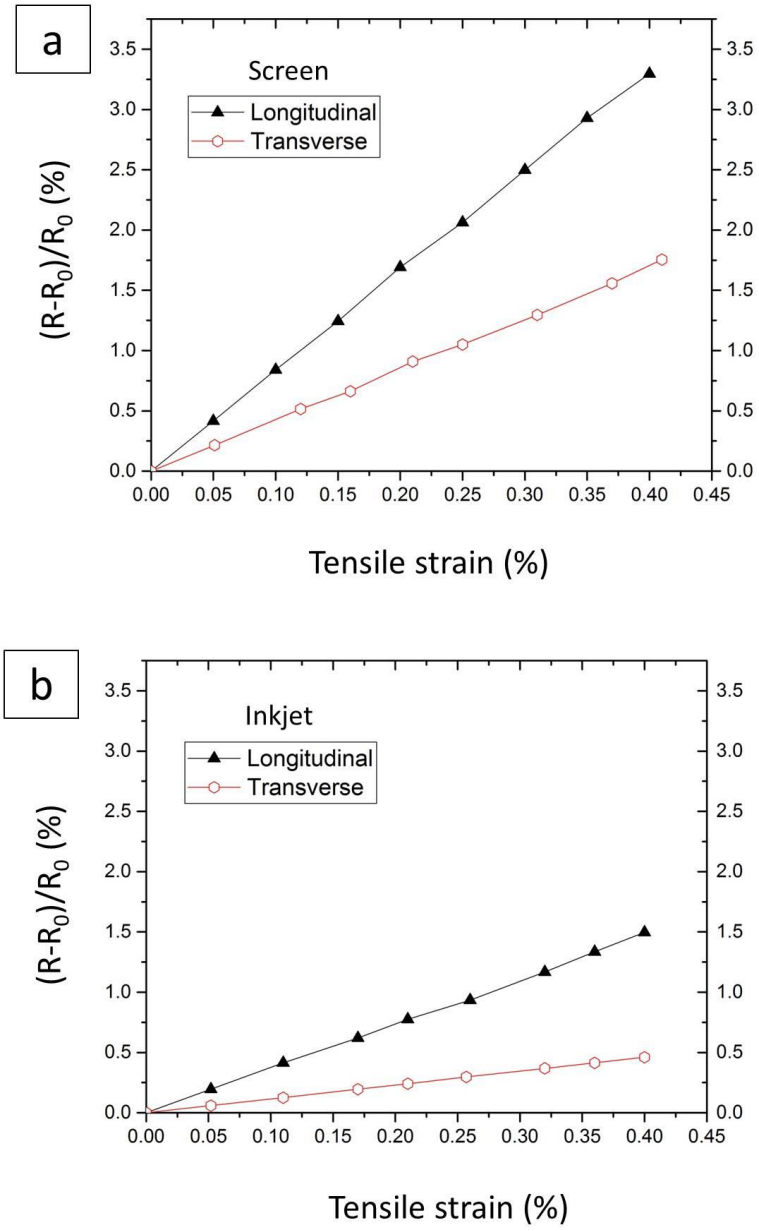

Figure 9. Sensor response curves in longitudinal and transverse directions for (a) the screen-printed and (b) the inkjet-printed sensors.

Please cite this article as: "All-printed Strain Sensors: Building Blocks of the Structural Health Monitoring System" Y Zhang, N Anderson, S Bland, S Nutt, G Jursich, and S Joshi, in press, Sensors and Actuators A, Oct (2016). DOI: 10.1016/j.sna.2016.10.007

Such high transverse sensitivities have been observed before for printed strain sensors [14], and are believed to be due to nature of polymeric materials used in printing processes. Increasing length-to-ratio may reduce the undesirable transverse sensitivity, as suggested by Table 2. This length-to-width ratio can be increased either by reducing the printing resolution or by scaling up the sensor size. The latter was not practical, since the sensor size would become too large to be useful in application. For screen printing, the minimum line width is limited by ink rheology and pattern mesh size whereas for inkjet printing it is limited by ink rheology and nozzle design. A major modification of the current printing techniques is required to achieve a line width reduction below ~100 μm. Furthermore, the transverse sensitivity issue can also be addressed by external circuit design in future studies.

Table 2. Transverse sensitivities and sensor geometries of screen-printed, inkjet-printed and commercial foil gages.

	Screen-printed gage	**Inkjet-printed gage**	**Commercial foil gage**
Transverse sensitivity	52%	31%	<1%
Gage length	8.1 mm	9.1 mm	6.5 mm
Line width	340 μm	180 μm	50 μm
Length to width ratio	24	51	130

3.5. Temperature sensitivity

A strain sensor is considered accurate if its gage factor is well-calibrated and the sensor is insensitive to all variables other than strain signal. A strain sensor relies on its resistance change as a response to applied strain. However, the resistance of the printed sensors was both time- and temperature-dependent at elevated temperatures. First, we found that the

Please cite this article as: "All-printed Strain Sensors: Building Blocks of the Structural Health Monitoring System" Y Zhang, N Anderson, S Bland, S Nutt, G Jursich, and S Joshi, in press, Sensors and Actuators A, Oct (2016). DOI: 10.1016/j.sna.2016.10.007

resistance of the screen-printed sensor varied as a function of time when held at a fixed temperature, as shown in Figure 10 (a). Such time-varying behavior made the temperature sensitivity of the sensor unpredictable, and thus we attempted to eliminate this time-varying resistance change which is believed to be caused by incomplete ink curing. Therefore, a prolonged curing at 120^{o}C for 2 hours was conducted after each print to remove the time-dependent resistance change (Figure 10 (b)). To prevent substrate bending during prolonged curing, the PET substrate could be annealed prior to printing in order to pre-stretch the substrate.

Please cite this article as: “All-printed Strain Sensors: Building Blocks of the Structural Health Monitoring System” Y Zhang, N Anderson, S Bland, S Nutt, G Jursich, and S Joshi, in press, Sensors and Actuators A, Oct (2016). DOI: 10.1016/j.sna.2016.10.007

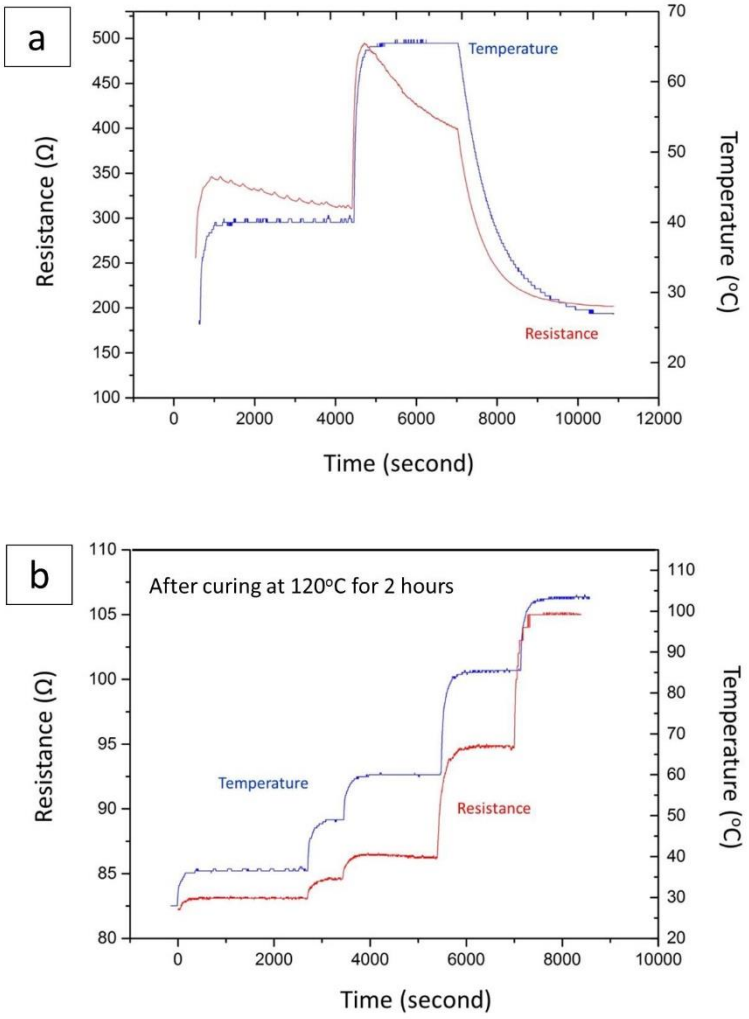

Figure 10. Time-dependence of the resistance change of the screen-printed sensor (a) before and (b) after prolonged curing at 120°C for 2 hours.

Second, the carbon-based resistive ink showed a positive temperature coefficient (PTC). This temperature-induced resistivity change was a result of electron-scattering and thermal expansion at elevated temperature. This phenomenon could lead to false strain reading called thermal output. To address this material problem, commercial foil gages utilize a

Please cite this article as: "All-printed Strain Sensors: Building Blocks of the Structural Health Monitoring System" Y Zhang, N Anderson, S Bland, S Nutt, G Jursich, and S Joshi, in press, Sensors and Actuators A, Oct (2016). DOI: 10.1016/j.sna.2016.10.007

constantan alloy (55% Cu-45% Ni) which has a small temperature coefficient (~10^{-5} K^{-1}) [15].

The temperature sensitivity of the screen-printed sensors must be investigated in order to predict the sensor performance in a temperature-varying environment. Two factors contributing to the thermal output are 1) resistivity change as a function of temperature [13], and 2) thermal stress due to sensor-substrate thermal expansion coefficient mismatch [16]. Therefore, the thermal output ε_{th}can be described by Equation 2,

$$\varepsilon_{th} = \frac{\alpha}{K} \cdot \Delta T + (\beta_s - \beta_i) \cdot \Delta T \quad \text{（Equation 2）}$$

where α is the temperature coefficient of resistance, K represents the gage factor, and $\beta_s$and β_i are the linear coefficients of thermal expansion of substrate and ink, respectively.

The temperature coefficient of resistance α was measured using a cured carbon ink block (50Ω at 300K) that was not attached to a substrate. Temperature was continuously recorded using a thermal couple and ink resistance was measured using a digital data logger. Figure 11 shows the resistance of the carbon block (50 Ω at 300 K) as a function of temperature. The temperature response curve was fitted by Equation 3.

Please cite this article as: “All-printed Strain Sensors: Building Blocks of the Structural Health Monitoring System” Y Zhang, N Anderson, S Bland, S Nutt, G Jursich, and S Joshi, in press, Sensors and Actuators A, Oct (2016). DOI: 10.1016/j.sna.2016.10.007

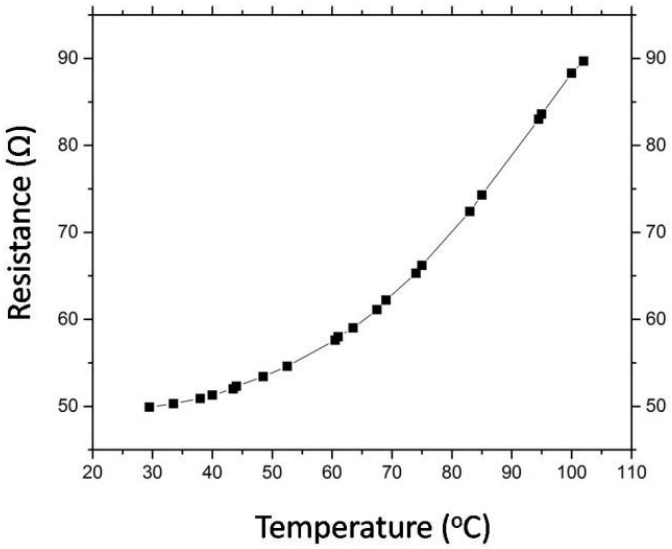

Figure 11. Resistance change of a free-standing carbon ink block as a function of temperature.

$$R(\Omega) = a_0 + a_1 \cdot T(℃) + a_2 \cdot T(℃)^2 \qquad \text{(Equation 3)}$$

where $a_0 = 56.3$, $a_1 = -0.43$, and $a_2 = 7.5 \times 10^{-3}$.

At room temperature, the temperature coefficient of resistance, α, of the carbon ink is 2.4×10^{-3} K^{-1}. The linear coefficient of thermal expansion is usually on the order of 10^{-6}~10^{-5} K^{-1} [17]. Therefore, the first term in Equation 2 (at least one order of magnitude larger than the second term) is the dominant factor of the temperature sensitivity of the carbon-ink sensors. The temperature sensitivity of the carbon ink is a material-related property and therefore must be compensated in calculations of strain by simultaneously using measured temperature data. Instead of looking for new ink materials, separating the thermal signal from the reading is a more practical and realistic approach. This can be

Please cite this article as: "All-printed Strain Sensors: Building Blocks of the Structural Health Monitoring System" Y Zhang, N Anderson, S Bland, S Nutt, G Jursich, and S Joshi, in press, Sensors and Actuators A, Oct (2016). DOI: 10.1016/j.sna.2016.10.007

achieved with a proximity temperature sensor as long as the temperature response of the printed sensors is well established as shown here.

Conclusions

Characteristics of printed strain sensors (gage factor, ink microstructure, temperature sensitivity, transverse sensitivity and fatigue response, etc.) are explored and compared with standard foil gages in this article. The printed sensors have significantly higher gage factors than standard foil gages and exhibited excellent linearity up to 0.4% strain with fatigue resistance up to 10^5 strain cycles. However, in order to employ these printed strain sensors in reliable structural health monitoring systems, their temperature and transverse-strain sensitivities need to be improved. These limitations result from the nature of these polymeric-based inks which can not easily be resolved in the near term, so future efforts will be directed toward post-signal processing algorithms using well characterized material property data. In addition, printing consistency with defect-free deposition and line resolution improvements will be further investigated in order to achieve reliable low-cost all-printed wide-area structural state sensing systems for practical applications. To realize a fully integrated strain mapping system, future efforts will also be dedicated to multiplexing electronics on flexible substrates as well as integration of a printed power source and conventional electronic integrated circuitry.

Please cite this article as: “All-printed Strain Sensors: Building Blocks of the Structural Health Monitoring System” Y Zhang, N Anderson, S Bland, S Nutt, G Jursich, and S Joshi, in press, Sensors and Actuators A, Oct (2016). DOI: 10.1016/j.sna.2016.10.007

Acknowledgements

The research and development presented in this publication is funded by the Office of Naval Research: Contract # N00014-14-C-0028. Authors acknowledge the technical monitoring of the project by Mr. William Nickerson. The views and conclusions contained in this document are those of the authors and should not be interpreted as representing the official policies, either expressly or implied, of the U.S. Navy. In addition, the authors would like to thank Bocheng Jin for his contribution to the MATLAB program. The authors would also like to thank the Nanotechnology Core Facility at UIC for the use of their class 10,000 cleanroom for screen printing.

References

1. G. Mattana and D. Briand, “Recent advances in printed sensors on foil,” *Mater. Today*, vol. 19, no. 2, pp. 88–99, 2015.
2. S. Wagner and S. Bauer, “Materials for stretchable electronics,” *MRS Bull.*, vol. 37, no. 03, pp. 207–213, 2012.
3. T. Duenas, S. Joshi, C. Del Solar, U.S. patent application number 20120031192, "Semiconductor strain gauge array", 2/9/2012.
4. L, Chang. "Piezoresistive Sensors", Pearson Prentice Hall. ISBN 0131472860, 2015
5. B. Ando and S. Baglio, “All-Inkjet Printed Strain Sensors,” *IEEE Sens. J.*, vol. 13, no. 12, pp. 4874–4879, 2013.

Please cite this article as: “All-printed Strain Sensors: Building Blocks of the Structural Health Monitoring System” Y Zhang, N Anderson, S Bland, S Nutt, G Jursich, and S Joshi, in press, Sensors and Actuators A, Oct (2016). DOI: 10.1016/j.sna.2016.10.007

6. Y. Wei, R. Torah, K. Yang, S. Beeby, and J. Tudora, “Screen printed capacitive free-standing cantilever beams used as a motion detector for wearable sensors,” *Procedia Eng.*, vol. 47, no. 0, pp. 165–169, 2012.
7. M. A. Alonso-Lomillo, O. Dominguez-Renedo, and M. J. Arcos-Martinez, “Screen-printed biosensors in microbiology; A review,” *Talanta*, vol. 82, no. 5, pp. 1629–1636, 2010.
8. S.Z. Chen, Q. Cai, F.Y. Peng, X.X. Huang, and Y.L. Jia, “Screen-Printed Electrochemical Biosensor for Detection of DNA Hybridization,” *Chinese J. Anal. Chem.*, vol. 40, no. 8, pp. 1194–1200, 2012.
9. B. Philip, E. Jewell, P. Greenwood, and C. Weirmann, “Material and process optimization screen printing carbon graphite pastes for mass production of heating elements,” *J. Manuf. Process.*, vol. Submitted, pp. 185–191, 2015.
10. M. Borghetti, M. Serpelloni, E. Sardini, and S. Pandini, “Mechanical behavior of strain sensors based on PEDOT:PSS and silver nanoparticles inks deposited on polymer substrate by inkjet printing,” *Sensors Actuators A Phys.*, vol. 243, no. 2016, pp. 71–80, 2016.
11. J. Herrmann, K. H. Muller, T. Reda, G. R. Baxter, B. Raguse, G. J. J. B. De Groot, R. Chai, M. Roberts, and L. Wieczorek, “Nanoparticle films as sensitive strain gauges,” *Appl. Phys. Lett.*, vol. 91, no. 18, pp. 7–9, 2007.
12. D. R. Cairns and G. P. Crawford, “Electromechanical properties of transparent conducting substrates for flexible electronic displays,” *Proc. IEEE*, vol. 93, no. 8, pp. 1451–1458, 2005.

Please cite this article as: “All-printed Strain Sensors: Building Blocks of the Structural Health Monitoring System” Y Zhang, N Anderson, S Bland, S Nutt, G Jursich, and S Joshi, in press, Sensors and Actuators A, Oct (2016). DOI: 10.1016/j.sna.2016.10.007

13. A. Garcia-Alonso, J. Garcia, E. Castano, I. Obieta, and F. J. Gracia, “Strain sensitivity and temperature influence on sputtered thin films for piezoresistive sensors,” *Sensors Actuators A. Phys.*, vol. 37–38, no. C, pp. 784–789, 1993.
14. V. Correia, C. Caparros, C. Casellas, L. Francesch, J. G. Rocha and S. Lanceros-Mendez, “Development of inkjet printed strain sensors,” *Smart Mater. Struct.*, vol. 22, No. 10, 2013.
15. J. R. Davis, Copper and Copper Alloys. ASM International. p. 158. ISBN 0-87170-726-8, 2001.
16. R. S. Okojie, A. A. Ned, and A. D. Kurtz, “Operation of alpha(6H)-SiC pressure sensor at 500 °C,” *Sensors and*, pp. 200–203, 1998.
17. F. Cverna, ASM Ready Reference: Thermal Properties of Metals, ASM International, ISBN: 978-0-87170-768-0, 2002.

Please cite this article as: “All-printed Strain Sensors: Building Blocks of the Structural Health Monitoring System” Y Zhang, N Anderson, S Bland, S Nutt, G Jursich, and S Joshi, in press, Sensors and Actuators A, Oct (2016). DOI: 10.1016/j.sna.2016.10.007